The application of dual-electrode through vial impedance spectroscopy for the determination of ice interface temperatures, primary drying rate and vial heat transfer coefficient in lyophilization process development

Geoff Smith*, Yowwares Jeeraruangrattana, Irina Ermolina

Journal	European Journal of Pharmaceutics and Biopharmaceutics
Date Submitted	March 3,2018
Date revised	May 16, 2018
Date Accepted	May 17, 2018

Cite as:

Smith, G., Jeeraruangrattana, Y. and Ermolina, I., 2018. The application of dual-electrode through vial impedance spectroscopy for the determination of ice interface temperatures, primary drying rate and vial heat transfer coefficient in lyophilization process development. European Journal of Pharmaceutics and Biopharmaceutics, 130, pp.224-235.

*Corresponding author

Leicester School of Pharmacy, De Montfort University, Leicester, LE1 9BH, United Kingdom

Abstract

Through vial impedance spectroscopy (TVIS) is a product non-invasive process analytical technology which exploits the frequency dependence of the complex impedance spectrum of a composite object (i.e. the freeze-drying vial and its contents) in order to track the progression of the freeze-drying cycle. This work demonstrates the use of a dual electrode system, attached to the external surface of a type I glass tubing vial (nominal capacity 10 mL) in the prediction of (i) the ice interface temperatures at the sublimation front and at the base of the vial, and (ii) the primary drying rate. A value for the heat transfer coefficient (for a chamber pressure of 270 μbar) was then calculated from these parameters and shown to be comparable to that published by Tchessalov (2017).

Keywords:

Freeze-drying; Lyophilization; Process analytical technology; Impedance spectroscopy; Dual electrode; Primary drying; Ice interface temperature; Heat transfer coefficient; dielectric relaxation of ice

1. Introduction

One of the dehydration techniques commonly used for drying of heat sensitive biopharmaceuticals, such as therapeutic proteins, is freeze drying or lyophilization. This multi-step process is costly, time-consuming and difficult to transfer technology from R&D scale to commercial scale manufacturing due to the differences in equipment scale/design and the impact of these factors on heat and mass transfer [2,3].

An example of the impact of scale, is that the proportion of the so-called 'edge' vials (i.e. those exposed to the radiant heat from the door and the walls of the primary drying chamber) to those considered to be core vials (i.e. those which are surrounded by vials at similar temperatures to each other) will be higher in the smaller dryer compared to the larger dryer, resulting in differences in the average drying rates of the two populations of vials.

One simple example of a difference in design is that a lab scale freeze dryer (which only has a capacity of 200-500 vials) often has an acrylic glass door which has a thermal radiation coefficient which is greater than that of the stainless steel doors used in the larger dryers (which can have capacities of up to 200,000 vials, depending on their size). It follows that the product temperature of the vials in the first few rows of a laboratory scale dryer (close to the chamber door) will be higher than the front row of vials in the commercial dryer [4] and therefore the former will again experience faster drying rates for the same freeze-drying protocol (e.g. shelf temperature set value).

Other factors associated with dryer design and scale are the distribution in shelf temperatures (both across an individual shelf and between shelves), the chamber pressure (especially the build-up of water vapor towards the center of the large shelves of a commercial dryer), the fill volume (or more specifically the fill height) and the product characteristics (such as dry layer resistance). Each and all of these have a direct influence on the distribution of product temperatures both within an individual vial and across the population of vials within the dryer. For example, the greater the fill height and the faster the drying rate (either because of a lower dry layer resistance and/or because the vial location

is close to the chamber wall) then the larger will be the temperature gradient from the bottom of the vial to the ice interface.

None of these issues would be so important, were it is not for the fact that an increase in product temperature above the glass transition of the freeze concentrated solution, T_g', may cause a collapse of the cake microstructure at a specific formulation related temperature known as collapse temperature, T_C. The possible consequences of exceeding the collapse temperature are reduced rates of drying (if collapse increases the dry layer resistance) and increased product temperatures (owing to reduce self-cooling rates). These factors can then impact the critical quality attributes of product stability, final moisture content and appearance, and even lead to the rejection of an entire commercial batch. In order to avoid such dramatic consequences, the product is usually dried at temperatures much lower than the theoretical limit, in order to maintain a safe margin between the product temperature and the collapse temperature but at the additional cost of a more prolonged primary drying time.

It is not surprising therefore that effort to improve process efficiencies have focused on the development and effective use process analytical technologies (PAT) for the determination of product temperature, as a significant process parameter [5-10]. These PATs can be divided into single vial techniques, which are characterized by having some forms of probe (usually inserted inside the vial) and batch techniques which are based on some direct or indirect measurement of drying rate from which mathematical models may be developed to predict the temperature at the ice sublimation interface (T_i) and at the base of the ice (T_b). It is not the intention here to fully appraise the strengths and weaknesses of currently available process analytical technologies as this information can be found in the recent reviews on process monitoring tools for pharmaceutical freeze drying [11-13].

1.1 Single Vial Techniques

Thermocouples (Type-T is generally used for pharmaceutical lyophilization) and resistance temperature detectors (abbreviated to RTD) are the traditional temperature sensors used for both

laboratory and production scale investigations. It is recommended that these sensors are positioned inside and at the center of the base of the vial where one expects the last vestiges of the ice mass will be removed [14]. To achieve this, it requires a fastening device to avoid the misplacement of the probe. The positioning of the sensor at the base of the vial is an appropriate strategy for witnessing the end point of primary drying and for determining the vial heat transfer coefficient (K_v) but less useful when trying to predict the closeness of the sublimation interface temperature (T_i) to the temperature at which the dry layer will collapse (T_c) when trying to drive process efficiencies using elevated shelf temperatures. For that application, it might be necessary to have two 'point' sensors positioned at two heights within the ice layer and to predict ice base and ice interface temperatures assuming a linear temperature gradient across the ice layer.

In primary drying, the heat absorbed at the sublimation interface creates a temperature gradient within the ice layer, such that the ice interface temperature (T_i) is lower than the base of the ice cylinder (T_b) by as much as 10 °C, depending on factors such as the drying rate and the height of the product being dried [8,15]. Both temperatures are of interest to the development scientist, as the base temperature (T_b) along with the shelf temperature allows one to calculate the heat transfer coefficient (provided the drying rate is known) whereas monitoring of the sublimation interface temperature (T_i) enables one to maintain the temperature of top layer product below the critical limit known as the collapse temperature, in order to ensure that the dry layer can maintain the porous structure and thereby facilitate vapour loss during both primary and secondary drying. If the target is to measure the temperature at the bottom of the vial (T_b) e.g. for end point determination or K_v calculations, then the thermocouple may suffice. However, if the target is to determine the ice interface temperature (T_i) using a thermocouple then it will be possible only during the initial period of drying owing to the fact that, once the top layer of ice has been removed, the thermocouple will lose contact and begin to sense the temperature of the gas above the ice layer rather than the layer itself. This is one of the incidental observations we have made in this study (see Fig. 10B in Section 3.5).

1.2 Batch Techniques

The first batch technique to be developed was the manometric temperature measurement (MTM) [6]. MTM combines data from the increase in pressure within the freeze drying chamber (that results from a transient closing of the isolation valve between the drying chamber and the condenser) with a mathematical equation to predict the 'batch average' temperatures at both the ice front and at the ice base within the vial. Some years following the introduction of MTM, Gieseler and coworkers [16] evaluated the potential of tunable diode laser absorption spectroscopy (TDLAS) for monitoring the sublimation rate during product development and process scale-up. Both MTM and TDLAS provide information on drying rates, as well as the temperatures at the base of the ice and at the sublimation interface, and so both techniques have been used successfully to characterize critical parameters of the system, such as heat transfer coefficients and dry layer resistances [6,16-21]. Both methods are also non-invasive methods and therefore won't alter the 'natural' characteristics and progression of the freeze-drying cycle. However, these techniques are limited in one sense, that they only provide a collective 'average' measurement of the batch and so if there is any significant heterogeneity in temperature and drying rates across the dryer and between shelves then these factors need to be accounted for in order to ensure that the process is modeled effectively. One way to account for this heterogeneity is to make certain assumptions concerning (i) the number of vials that can be considered as edge vials in proportion to the overall size of the batch, and (ii) the impact of radiant heating; and to introduce factors which model the faster drying rates of these vials [1]. An alternative and indeed complimentary approach would be to combine a non-invasive batch method such as MTM or TDLAS with a number of single measurements in the edge vial populations. An example of this approach is the "LyoMonitor" which multiplexes data from MTM and thermocouples in order to control the primary drying cycle [22].

Returning to a consideration of the single vial approaches, there appears to be a gap in the market for a sensor which can determine the ice interface temperature and the ice base temperature in a single vial (in a non-invasive manner) but is also able to measure the drying rate in a way that

doesn't interfere with the hexagonal packing of the vials (as would be the case if using a microbalance to determine drying rates). Such a device could be deployed at key locations in the dryer and then multiplexed with MTM or TDLAS in order to qualify and validate the batch models which have incorporated factors for batch heterogeneity.

1.3 Through-vial impedance spectroscopy (TVIS)

TVIS has been developed in the first instance as a non-invasive process analytical technology for determining critical process parameters within individual vials, at user-defined locations across a small scale development dryer. The basis for the TVIS technology is the measurement of the electrical impedance of a freeze-drying vial containing the product, i.e. the opposition to current flow when an alternating voltage is applied to the vial, using a pair of electrodes which are attached to the external surface of the glass wall (hence the term "through-vial"). With a through vial impedance measurement it is the changes in the electrical properties of the composite object (comprising the product and the glass wall) that reflect the physical condition of the product during the freeze drying process [23]. Using a simple empirical approach in the first instance (as opposed to more sophisticated modeling of the electrical behavior of the composite object) it is possible to extract useful information about the sublimation of ice from the amplitude (C''_{PEAK}) and characteristics frequency (F_{PEAK}) of the dielectric loss peak that results primarily from the dielectric relaxation of ice. The C''_{PEAK} parameter is sensitive to the height of the ice cylinder within the electrode space (i.e. the internal volume of the vial which is bounded by the external electrodes) from which one can predict the rate of primary drying, whereas the F_{PEAK} parameter can be calibrated through the incorporation of an annealing stage and then used to predict the product temperature in a subsequent primary drying stage [24]. Both parameters also lend themselves to the determination of phase behavior (e.g. ice formation and eutectic formation) [25,26].

1.4 Study Aim

The aim of this study is to develop the application of TVIS for predicting the two ice interface

temperatures (at the sublimation front and the bottom of a conventional glass tubing vial) while simultaneously quantifying the primary rate, so as to deliver all the parameters required for the estimation of the heat transfer coefficient, according to the method described first by Pikal, Roy and Shah [27].

2. Materials and Methods

2.1 Measurement Principles

In this study, we report for the first time, the use of a dual electrode system comprising two pairs of copper electrodes attached to the outer surface of an Adelphi VC010-20C Type I glass tubing vial, with one large electrode pair enveloping the ice interface region and one smaller electrode pair closer to the base of the vial. The bottom electrode (BE) has height-by-width dimension of 5 × 19 mm and is positioned 3 mm above from the base of the vial whereas the top electrode (TE) has a height-by-dimension of 15 × 19 mm and positioned 3 mm from the top edge of bottom electrode (and therefore 11 mm from the base of the vial) (Fig. 1)

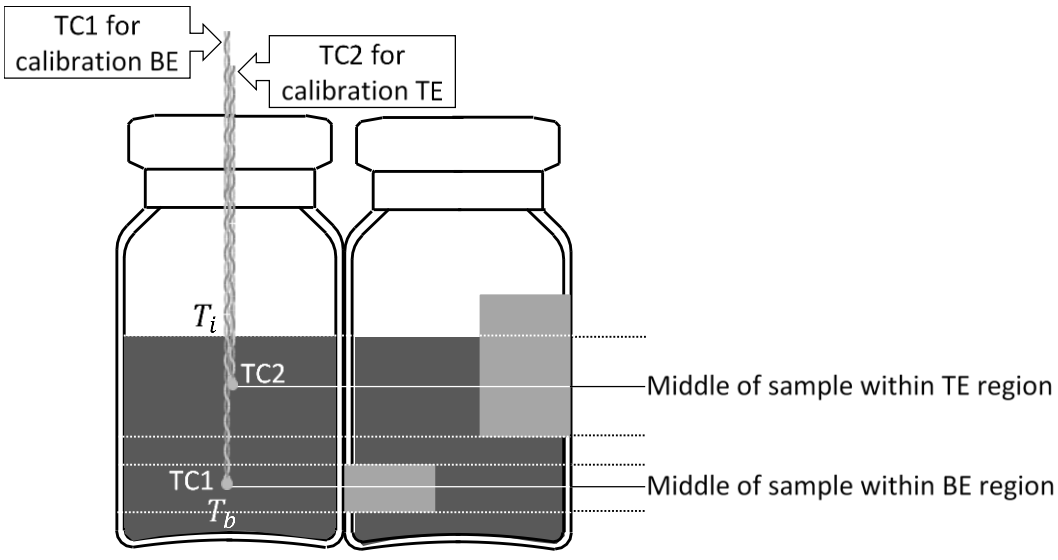

Figure 1. Method for calibrating the temperature response the TVIS system using a dual pair of electrode. LEFT : Standard type I glass tubing vial (Adelphi VC010-20C of nominal volume 10 mL)with two type-T thermocouples placed at height which are equivalent to the center points of the upper and lower electrodes; RIGHT : a TVIS modified vial with two pairs of copper foil electrodes (only one electrode from each pair is shown here).

The TVIS measurement vial is connected via a junction box inside the freeze-dryer and via a bespoke pass-through (attached to the manifold) to a five channel impedance analyzer which has been developed by De Montfort University [28]. The impedance spectra from each electrode pair was measured across the frequency range of 10 Hz to 1MHz at an interval of every 2 min throughout the entire freeze-drying cycle. The time to acquire each individual spectrum was of the order of 10 seconds. The peak frequency (F_{PEAK}) and peak amplitude (C''_{PEAK}) of the main process was then determined by a simple peak finding routine that was built in as a feature of our LyoView™ analytical software (Fig. 2).

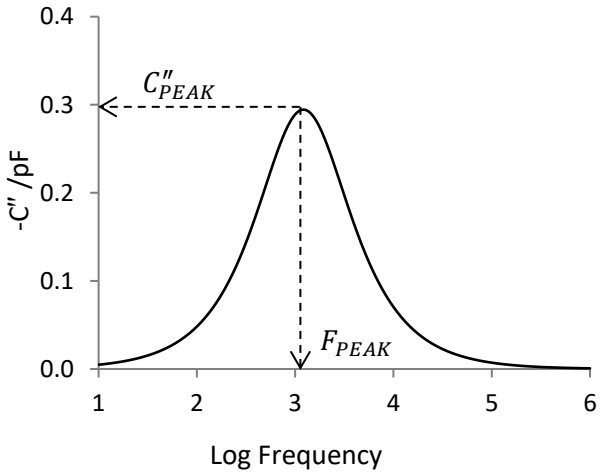

Figure 2. Example model spectrum to demonstrate the determination of F_{PEAK} and C''_{PEAK} values.

We have shown in a previous article [23] that the parameter F_{PEAK} is sensitive to the average temperature of the ice in the region bounded by the electrodes whereas the parameter C''_{PEAK}, whilst it also has a smaller dependency on temperature, is largely sensitive to the height of the ice cylinder in the region bounded by the electrodes. We also recognize here that the relationship between the magnitude of C''_{PEAK} and the height of the ice layer is only linear if there is intimate contact between the ice and the inside wall of the glass vial (i.e. no gaps appear during drying) and that the ice dries as a cylinder without any change in the shape of the sublimation interface. This might, at first present as a disadvantage of the technique in terms of its generalized ability to measure the sublimation rate

throughout the primary drying stage. However, in all methods for the determination of K_v, there is an expectation that the drying rate is determined from a limited period of the primary drying stage, either by gravimetric measurements of mass lost after a truncated period of drying or by some real time monitoring technique, such as TDLAS or MTM. This is to ensure that the heat transfer mechanisms from the head space above the ice layer and from the side walls do not change because of some changes in the shape of the sublimation front or the contact between the ice cylinder and the wall of the vial. Here we can demonstrate that it is possible to use the TVIS technique to define the period over which the ice layer maintains contact with the glass wall and thereby derive a reliable estimate of K_v

There are a number of stages to this new TVIS method: The **first stage** is to record F_{PEAK} values from both electrode pairs, during a slow temperature ramp of pre-frozen water, which spans the temperature range of interest for subsequent primary drying (in our case −40 to −15 °C). Given that F_{PEAK} is a function of the average ice temperature in the region bounded by a single electrode pair [23] then it's possible to calibrate the two values of F_{PEAK} from each electrode pair against the two temperatures which are centered at specific heights within the ice cylinder. To make the calibration, the nearest neighbor vial has two 30 AWG thermocouples positioned at heights that correspond to the center points of ice cylinders within each electrode pair in the TVIS vial (Fig. 1). The positioning of the thermocouples required careful manual manipulation by inserting them through a very small hole in rubber stopper. A process of trial and error, with visual observations from multiple angles was use to qualify the central positioning of the thermocouple tip. The choice of the thicker 30 AWG thermocouple as opposed to those recommended by Nail 2017 [12] (i.e. 36 AWG) provided some rigidity to the probe which helped maintain the location of the probe once the positioning process was completed. Unfortunately, the insertion of a 'grounded' thermocouple within the TVIS vial results in a dramatic distortion of the spectrum to such an extent that in effect renders the spectrum unusable. The calibration function, which is based on a second order polynomial, then provides the basis for the prediction of product temperatures during the subsequent primary drying step. The

predicted primary drying temperatures will be referred to as $T_{(F_{PEAK})}$ given that they are derived from the TVIS parameter, F_{PEAK} (see Section 3.1).

The **second stage** is to standardize values of C''_{PEAK} (that have been recorded during the primary drying stage) to a reference temperature of −20 °C, in order to compensate for the small temperature dependency of this parameter (see Section 3.2). The standardized peak amplitude is given by $\hat{C}''_{PEAK}$, i.e. with a circumflex over the letter C.

The **third stage** is to calibrate values of C''_{PEAK} recorded at the reference temperature of against known fill heights of ice occupying the internal volume of the vial that is bounded by the top electrode pair and then use the calibration factor to convert the rate of change of the standardized peak amplitude ($\hat{C}''_{PEAK}$) to a drying rate (see Section 3.3).

The **fourth stage** is to use the methodology developed in Section 3.3 to determine the position of the ice interface and then extrapolate from the predicted temperatures at the two known vertical positions (within the volumes bounded by the two pairs of electrodes) to the relative positions of the ice interface and ice base, respectively, in order to predict values for the temperatures at the sublimation front (T_i) and the base of the ice (T_b) (see Section 3.4).

2.2 Loading the freeze-dryer

8.12 g aliquots of 18 MΩ.cm water were transferred to one hundred and sixty Adelphi VC010-20C type I glass tubing vials (one of which was modified for our dual electrode TVIS measurements, as described in see Section 2.1). For the TVIS vial, this amount of water corresponds to a fill factor (Φ) of 0.7 for the top electrode pair (where Φ is defined as the relative height of the liquid bounded within electrode region to the height of the top electrode). Each vial was then plugged loosely with a 20 mm 4023/50 bromobutyl grey rubber stopper FDW20RTS (West Pharmaceutical Services Singapore Pte. Ltd, Singapore) and weighed to a precision of 3 decimal places, in order to determine the gross weight of each vial prior to commencing the freeze drying cycle. The vials were then loaded into the drying chamber of a VirTis AdVantage Plus bench-top freeze dryer according to the schematic shown in Fig.

3. The TVIS vial is placed at the center of the shelf with one of the nearest neighbor vials having a pair of type T thermocouples inserted through the rubber stopper and with the sensing beads positioned at the two specific heights as shown in Fig. 1

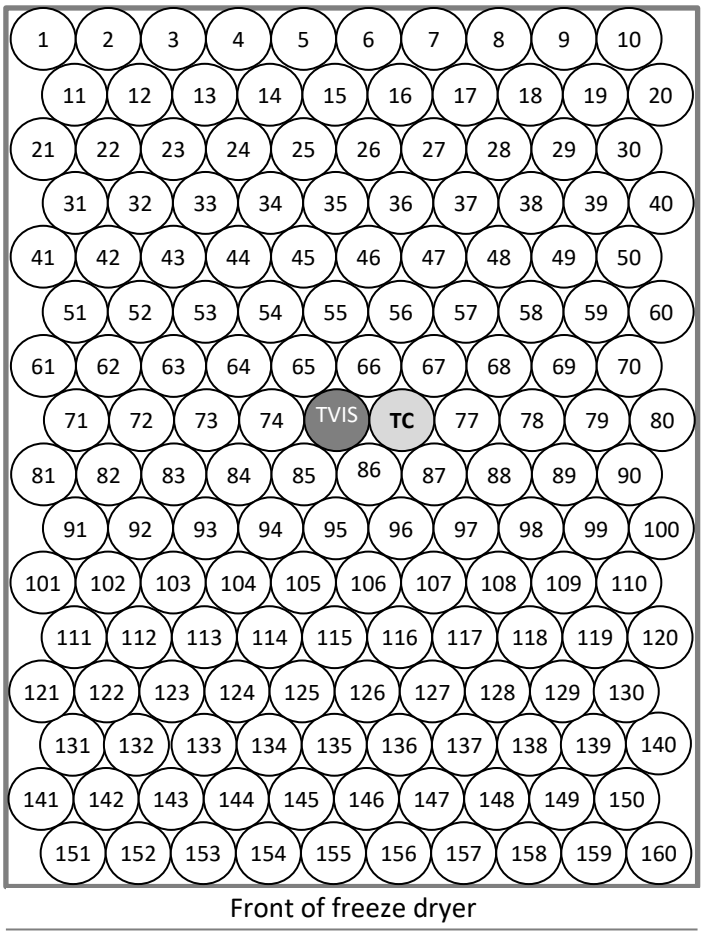

Figure 3. Arrangement of vials on the middle shelf of a VirTis AdVantage Plus freeze-dryer. The two vials at positions 75 and 76 are the TVIS modified vial and the thermocouple containing vial.

2.3 Freeze-drying protocol

A freeze drying protocol (Table 1) with a re-heating step (subsequent to the first freezing of ice) and an interrupted primary drying stage (to be able to quantify the ice mass remaining in the vial) was designed with the purpose of being able to validate the predictions of the ice interface

The inclusion of the ramp in shelf temperature from −40 to 0 °C while maintaining the chamber pressure at ~ 270 µbar (as recorded by the pressure gauge) will create an 'activation point' where the ice interface temperature approaches T_i = −33.2 °C; which is a temperature at which the

ice interface partial pressure exceeds the chamber pressure ($P_i \geq P_c$) causing the drying rate to increase dramatically. This 'activation point' may be determined from the point, during the temperature ramp, when the rate of change of C''_{PEAK} from the top electrode increases more significantly.

Table 1. Freeze drying protocol. Note that, in practice, the set pressure of 350 µbar translated to an actual chamber pressure of 270 ± 15.4 µbar during the process of primary drying.

Step	**Temperature (°C)**	**Time (minutes)**	**Cumulative Time (minutes)**	**Set pressure (µbar)**
Equilibrium phase	+20	10	10	-
Freezing temperature ramp (0.5 °C /min)	−45	130	140	-
Freezing temperature hold	−45	180	320	-
Re-heating temperature ramp (0.5 °C /min)	−10	70	390	-
Re-heating temperature hold	−10	120	510	-
Re-cooling temperature ramp (0.5 °C /min)	−40	60	570	-
Re-cooling temperature hold	−40	120	690	-
Primary drying temperature hold	−40	30	720	350
Primary drying temperature ramp (0.5 °C /min)	0	80	800	350
Primary drying temperature hold	0	250	1050	350

The other essential feature of the cycle was that it was designed (following initial exploratory studies) to interrupt the primary drying process when only ~20% of the ice has been removed; in our case when the ice cylinder height is reduced from 20.5 to 16.7 mm. This reduction in ice cylinder height can be expressed in terms of the fill factor for the top electrode decreasing from 0.7 to 0.45 and so we can expect that the C''_{PEAK} parameter will have a linear dependency on ice mass (as demonstrated in Section 3.3) provided the profile of the ice interface does not change. All vials were removed from the freeze dryer after the primary drying process was interrupted and then re-weighed. The mass of water loss during the freeze-drying run was then calculated and an average drying rate determined from the difference in mass divided by the time elapsed. This drying rate provides one opportunity to qualify the use of the standardized peak amplitude ($\hat{C}''_{PEAK}$) for determining the mass of ice remaining within the vial (See results in Section 3.5).

3. Results

3.1 Ice temperature calibration

Temperature calibration for each electrode pair is achieved by plotting the temperatures ($T_{(TC)}$) from the thermocouple sensing probes in the nearest neighbor vial (those that were acquired during the temperature ramp at the slow rate of 0.5 °C·min^{-1} at the heights equivalent to the center points within the two pairs of electrodes, against the F_{PEAK} values for corresponding time point at which each temperature was recorded and then fitting a 2nd order polynomial function (Fig. 4). See Table 2 for the polynomial coefficients for the top and bottom electrodes.

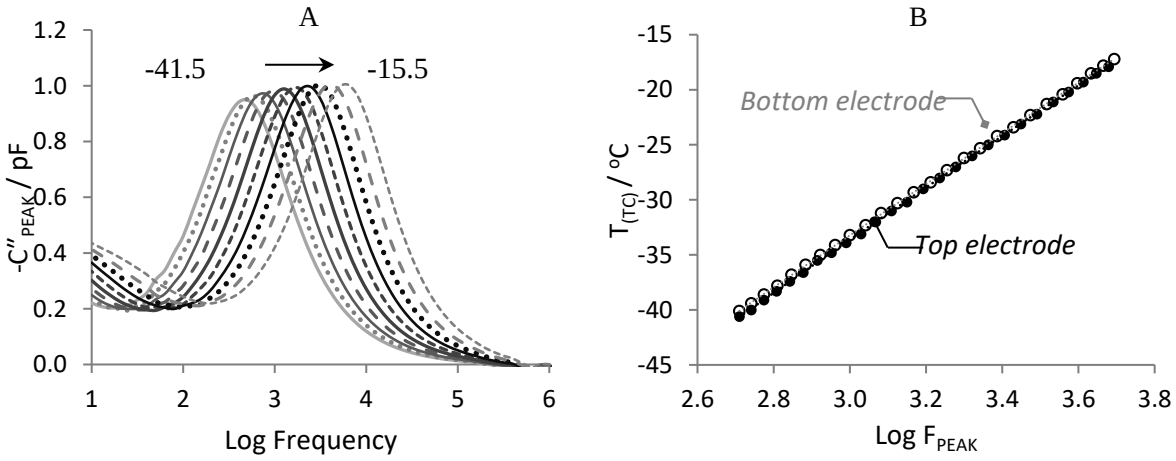

Figure 4. (A) Selection of imaginary capacitance spectra of ice from the top electrode pair of the TVIS vial, during the reheating ramp from −40 to −15 °C; (B) Calibration plots from the re-heating stage for the prediction of ice interface temperatures from estimates of F_{PEAK} measured during the subsequent primary drying stage.

Table 2. The calibration coefficients from the re-heating of ice: To be used for the prediction of temperatures from measurements of F_{PEAK} during the primary drying stage.

Order of the fitting coefficient	2 (a)	1 (b)	0 (c)
Temperature coefficient-TE	-1.02	30.1	-115
Temperature coefficient-BE	-5.43 x 10^{-4}	26.7	-109

3.2 Temperature compensation for C''_{PEAK}

The temperature dependency of C''_{PEAK} (which is observed during the re-heating part of the thermal cycling phase) is inevitably manifest in the primary drying stage, which means that the time

dependency of C''_{PEAK} during primary drying cannot be wholly attributed to the loss of ice. Any change in temperature will also impact the value of C''_{PEAK} and so in order to compensate for temperature, a standardization factor (Ø) is calculated which can be used to temperature normalize all values of C''_{PEAK} to that obtained if the temperature was fixed at some reference value. In our case we have chosen a temperature of –20 °C as the reference value.

$$\emptyset(T) = \frac{C''_{PEAK}(T)}{C''_{PEAK}(-20)} \quad (1)$$

Here, $C''_{PEAK}(T)$ and $C''_{PEAK}(-20)$ are the peak amplitudes at temperatures T and −20 °C, respectively, during the re-heating ramp. Typically, the temperature dependency of C''_{PEAK} which is determined during the re-heating stage, can be modelled with a 2nd order polynomial over a limited temperature range of interest (e.g. −45 to −15 °C) which means that Eq. (1) may be re-written in terms of the polynomial coefficients determined in Section 3.1 (Eq. (2))

$$\emptyset(T) = \frac{aT^2 + bT + c}{aT_o{}^2 + bT_o + c} \quad (2)$$

where T is the center point temperature from the top electrode ($T_{(F_{PEAK})TE}$) at time t during the primary drying phase, and T_o is the reference temperature of −20 °C. Values for the polynomial coefficients are given in Table 2.

Values for $C''_{PEAK}(T,t)$ at any time (t) and temperature (T) during the primary drying stage are then adjusted by dividing each value by the calibration factor (Ø) to give temperature standardized values $\hat{C}''_{PEAK}(-20,t)$. Note the use of the circumflex to indicate that these values are the standardized values at time *t* during the primary drying stage

Fig. 5A shows the temperature dependency of C''_{PEAK} as determined during the re-heating cycle, and Fig. 5B shows the uncompensated C''_{PEAK} values and the standardized $\hat{C}''_{PEAK}$ values (doted and solid lines respectively) of as a function of primary drying time. One should notice that the standardized $\hat{C}''_{PEAK}(-20,\mathrm{t})$ values are almost constant until approximately 1.5 h, whereas the

uncompensated values reflect the impact of the start of the heating ramp at 30 min.

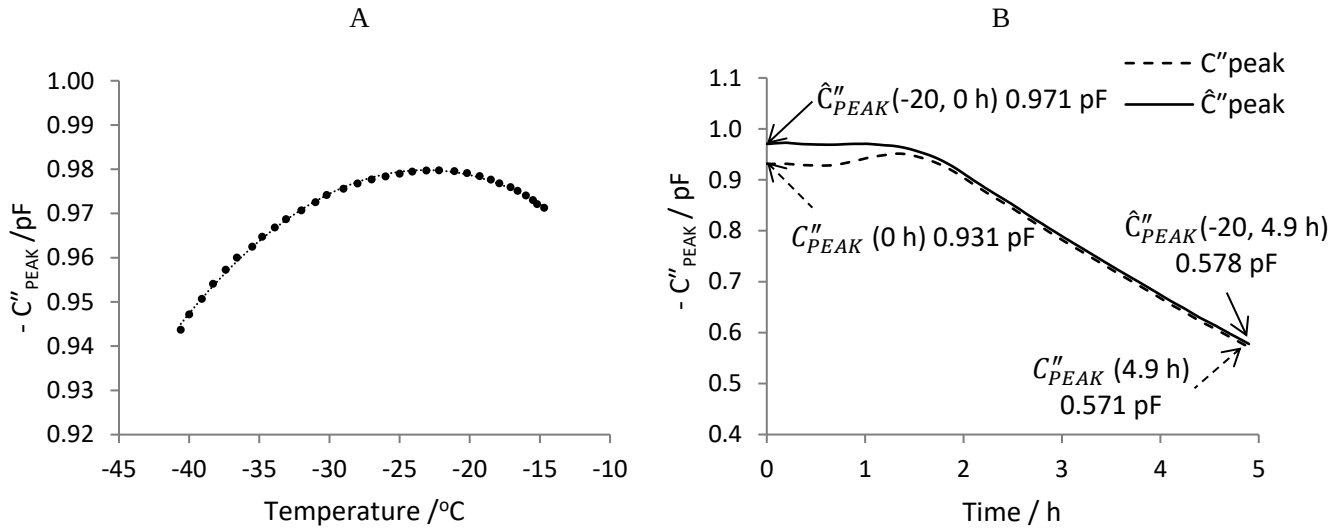

Figure 5. (A) The temperature dependency of C''_{PEAK} for the top electrode and (B) values for C''_{PEAK} during primary drying, before and after correction for temperature. Note that the nomenclature of the corrected value of the peak height ($\hat{C}''_{PEAK}(-20,t)$).

3.3 Primary drying rate determination

Once C''_{PEAK} has been corrected for temperature by standardizing all values to a reference temperature, T_o (in our case, T_o = −20 °C) then it is possible to derive a $\hat{C}''_{PEAK}(-20,t)$ based surrogate for the sublimation rate from the difference between $\hat{C}''_{PEAK}(-20,t)$ at two time points ($t2$ and $t1$) according to the following equation

$$\frac{\Delta \hat{C}''_{PEAK}}{\Delta t} = \frac{\hat{C}''_{PEAK}(-20,t2) - \hat{C}''_{PEAK}(-20,t1)}{t2 - t1} \qquad (3)$$

After defining the surrogate primary drying rate (in terms of the rate of change of the standardized values of $\hat{C}''_{PEAK}(-20,t)$ (Eq. (3)) it is then possible to calculate an actual drying rate (in units of g/h for example) by studying the equivalence between C''_{PEAK} and ice mass through the separate experiment in which a range of fill heights of ice are measured at a fixed reference temperature (in our case −20 °C).

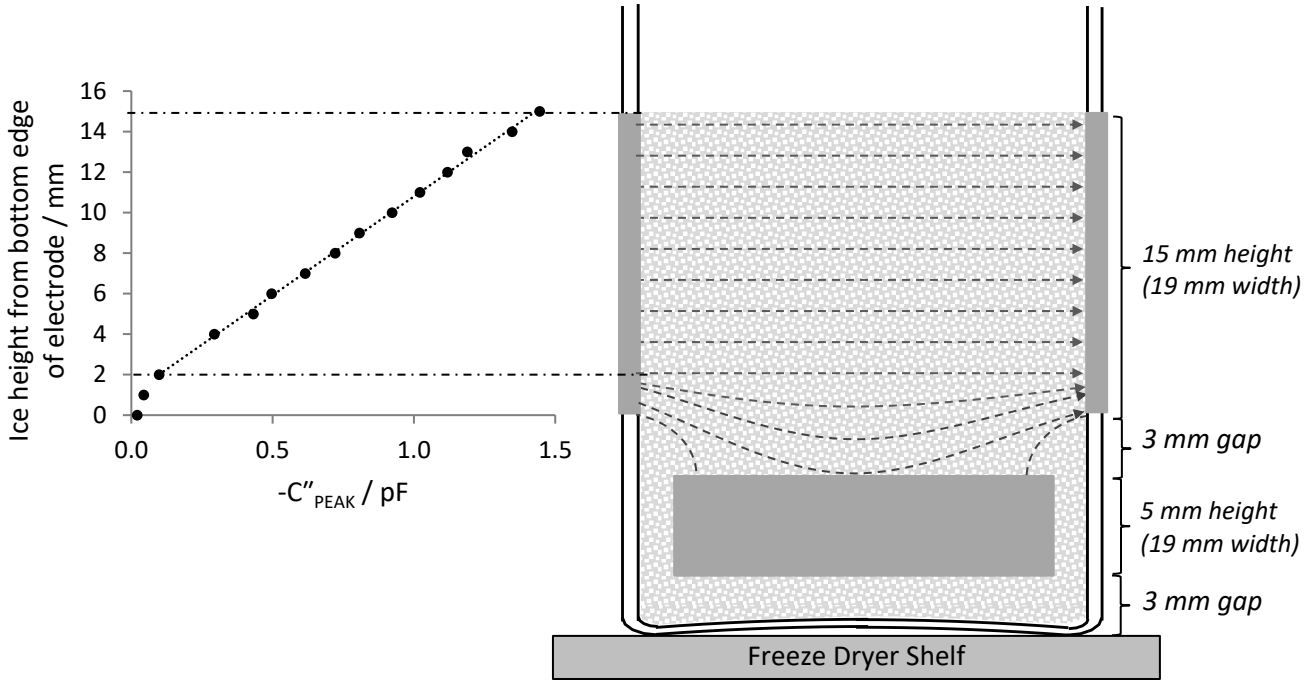

Figure 6. The dependency of C''_{PEAK} on the ice cylinder height in the region bounded by the top electrode. The gradient of the linear portion of the graph ($m_{h/C}$) at fill heights from the bottom edge of the top electrode which are greater than 2 mm, is equal to 9.749 mm/pF (0.975 cm/pF) and provides the calibration factor to convert rates of change in C''_{PEAK} to values of the ice mass during primary drying.

The non-linear portion of the graph (Fig. 6) between fill heights from zero (where the ice interface just reaches the bottom edge of top electrode) to approximately 2 mm is the result of the non-linear field at the periphery of the lower edge of the top electrode. At fill heights greater than 2 mm there is a linear relationship between C''_{PEAK} and fill height and so the gradient of the line ($m_{h/C}$) provides the calibration factor which can be used to convert the rate of change of $\hat{C}''_{PEAK}$ ($\Delta\hat{C}''_{PEAK}/\Delta t$) in the primary drying phase to the rate of change of ice cylinder height ($\Delta h/\Delta t$).

$$\frac{\Delta h}{\Delta t} = m_{h/C} \cdot \frac{\Delta\hat{C}''_{PEAK}}{\Delta t} \qquad (4)$$

Assuming that the ice interface area remains unchanged during the truncated primary drying period of this experiment then the change in ice cylinder height (h) in the region bounded by the top electrode can be equated to a change in volume (m) by simply multiplying Eq. (4) by the internal cross sectional area of the vial (A) and the density of ice (ρ_i) at the steady state temperature when

the drying rate is constant.

$$\frac{\Delta m}{\Delta t} = \rho_i \cdot A \cdot \frac{\Delta h}{\Delta t} = \rho_i \cdot A \cdot m_{h/C} \cdot \frac{\Delta \hat{C}''_{PEAK}}{\Delta t} \quad (5)$$

It follows from Eq. (5) that any change in C''_{PEAK} due to the receding ice layer can be converted directly to drying rate, provided the electrode pair is first calibrated with known heights of ice within the electrode space.

3.4 Prediction of ice interface and ice base temperatures

Once the calibration of $Log\ F_{PEAK}$ has been undertaken during the temperature ramp on ice (Section 3.1) then the calibration coefficients for the 2nd order polynomial fit of temperature against $Log\ F_{PEAK}$ (Table 2) can be used to predict the primary drying temperatures at the center points of the ice cylinders in each of the regions bounded by the top and bottom electrode, i.e. $T_{(F_{PEAK})TE}$ and $T_{(F_{PEAK})BE}$, respectively. However, in order to achieve the ice temperature at sublimation front, one first needs to know the position (i.e. height) of the sublimation interface in relation to the three reference points, i.e. the two center points of the electrodes and the interface between the bottom of the ice and the base of the vial. The height of the sublimation interface can be determined from the linear relationship between $\hat{C}''_{PEAK}$ (i.e. the compensated value of C''_{PEAK} at the reference temperature of −20 ˚C that was established in Section 3.3) and the height of ice cylinder bounded by the top electrode (Eq. (6)) coupled to the height of the bottom edge of the top electrode from the inside base of the vial (Fig. 7)

$$The\ ice\ height = 9.7485 \times \hat{C}''_{PEAK} + 1.0462 \quad (6)$$

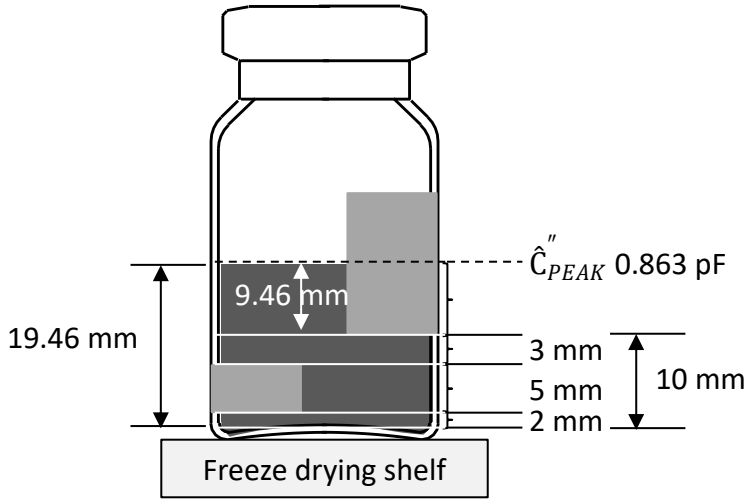

Figure 7. Illustration of the calculation of the ice height at 2.4h into the primary drying stage for an Adelphi VC010-20C type I glass tubing vial

For example, at 2.4 h into primary drying the temperature compensated peak amplitude ($\hat{C}''_{PEAK}$ at −20 °C) is 0.863 pF; therefore from Eq. (6) the ice height within the top electrode region is 9.46 mm. Add to that the distance between the inside base of the vial and the bottom of the top electrode (i.e. 10 mm) then gives a sublimation front at 19.46 mm from the inside base of the vial.

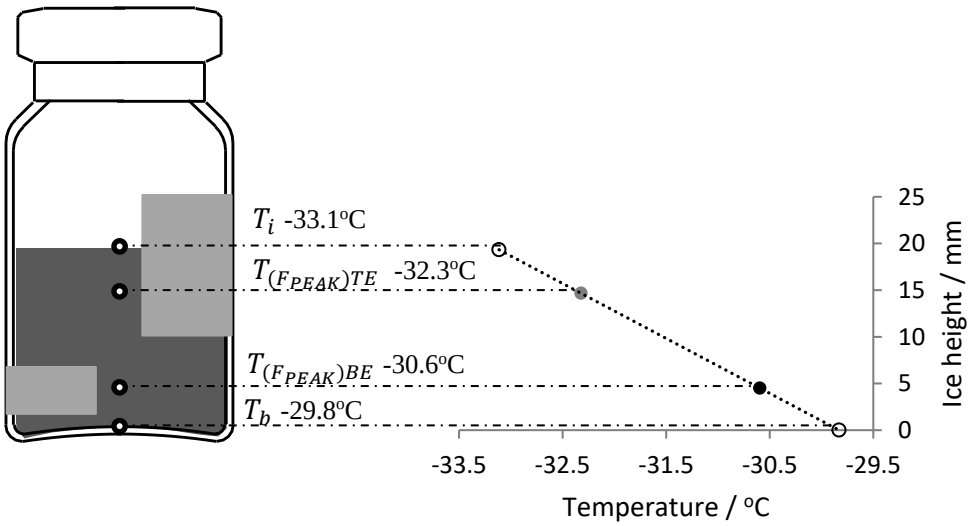

Figure 8. A 2 point-temperature determination for extrapolation to the ice interface temperatures of interest (i.e. T_i and T_b). The example shown here is from 2.4 h into primary drying (during the steady state period).

Fig. 8 shows an example to illustrate how this methodology is applied. In effect, one plots the two temperatures at the known positions of the center points of the upper and lower electrode pairs

and then one assumes that the temperature gradient up the ice layer is linear so that one can then extrapolate to the base interface (at an ice height of zero) and to the sublimation front interface (at an ice height determined from Eq. (6) plus the height of the lower edge of the top electrode from the inside base of the vial).

By applying this methodology across the primary stage (by using values of $\hat{C}''_{PEAK}$ corresponding to each time point) one can account for the changing position of the ice interface within the region bounded by the top electrode and follow the ice interface temperatures at both the sublimation front and at the base of the ice.

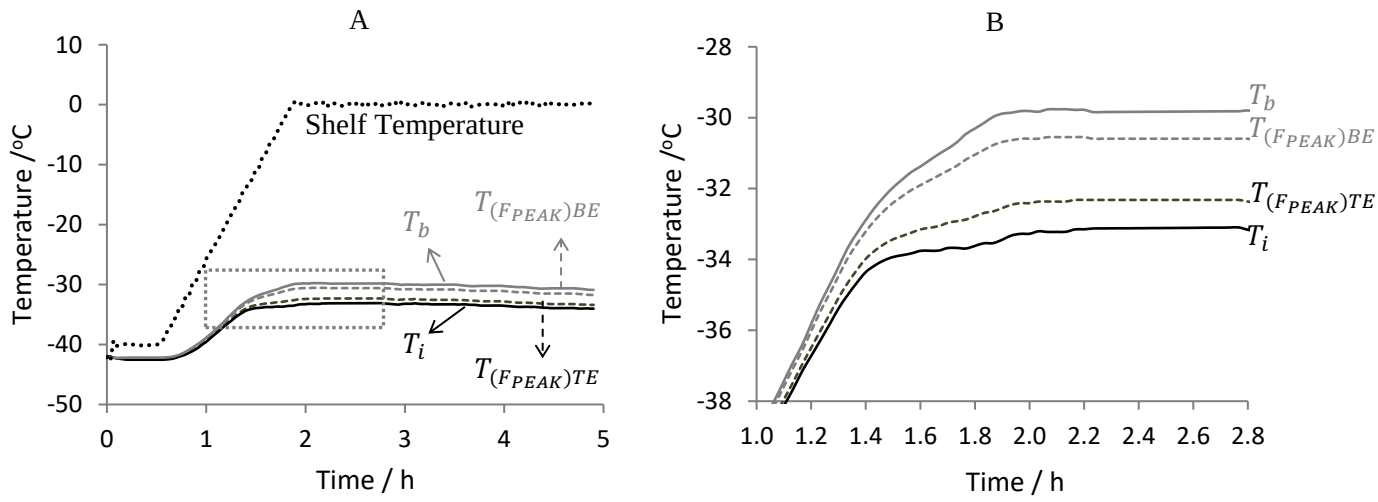

Figure 9. Predicted ice interface temperatures at the sublimation front (T_i) and the base of the ice (T_b), during the first 5 hours of primary drying (as determined by the extrapolation from the TVIS predicted temperatures at the center of the top and bottom electrode spaces.

Fig. 9A shows $T_{(F_{PEAK})}$ values for the top and bottom electrodes and the predicted temperatures values for the ice interfaces at the sublimation front and at the bottom of the vial (T_i and T_b respectively). Fig. 9B shows the enlarged scale in order to illustrate that there is a period of steady state (between 2 and 2.8 h) when the temperature is constant (i.e. does not drift by more than 0.2 °C) and so we would expect the drying rate to be constant also (see Fig. 10D in Section 3.5).

3.5 Qualification of the ice interface temperature prediction

As predicted, the inclusion of the ramp in shelf temperature from −40 to 0 °C while maintaining the chamber pressure at ~ 270 μbar causes the drying rate (as evidenced by the rate of change of $\hat{C}''_{PEAK}$ values associated with the top-electrode) to increase dramatically because the sublimation interface temperature is approaching the activation point, where the partial pressure of ice will be not less than the chamber pressure ($P_i \geq P_c$) (Fig. 10D).

Fig. 10A shows the theoretical relationship between ice interface temperature and the partial pressure of ice, with the horizontal dashed lines showing the limits of uncertainty in the partial pressure of the chamber (and therefore the minimum anticipated partial pressure of ice required for sublimation to occur) that resulting from the fluctuation in the measured values of partial pressure, 270 ± 15.4 μBar. Following those pressure limits, in terms of the equivalent ice interface temperatures, across to the plot of predicted ice interface temperature vs primary drying time (Fig. 10B) demonstrates that when the ice interface temperature, and therefore pressure, approaches the lower limit of uncertainty in the chamber pressure then there is a change in the trajectory of the ice interface temperature as a result of the self-cooling mechanism that accompanies the activation of primary drying. On closer inspection of the inflection in the trajectory of the predicted ice interface temperature (Fig. 10C) suggests that the activation of primary drying coincides with an ice interface temperature of – 34 °C. This activation process is confirmed by a more rapid rate of change in the value of $\hat{C}''_{PEAK}$, which is the parameter that directly relates to the amount of ice remaining within the region bounded by the top electrodes (Fig. 10D).

Another observation from Fig. 10 is that the rate of change of $\hat{C}''_{PEAK}$ continues to increase as the temperature ramps further towards its set temperature of 0 °C; after which the ice interface temperature remains stable at −33.1 °C; This value is close to the ice interface temperature of −33.2 °C that would be predicted from the equivalence between the partial pressure of ice and the chamber pressure during activated drying ($P_i \geq P_c = 270$ μbar).

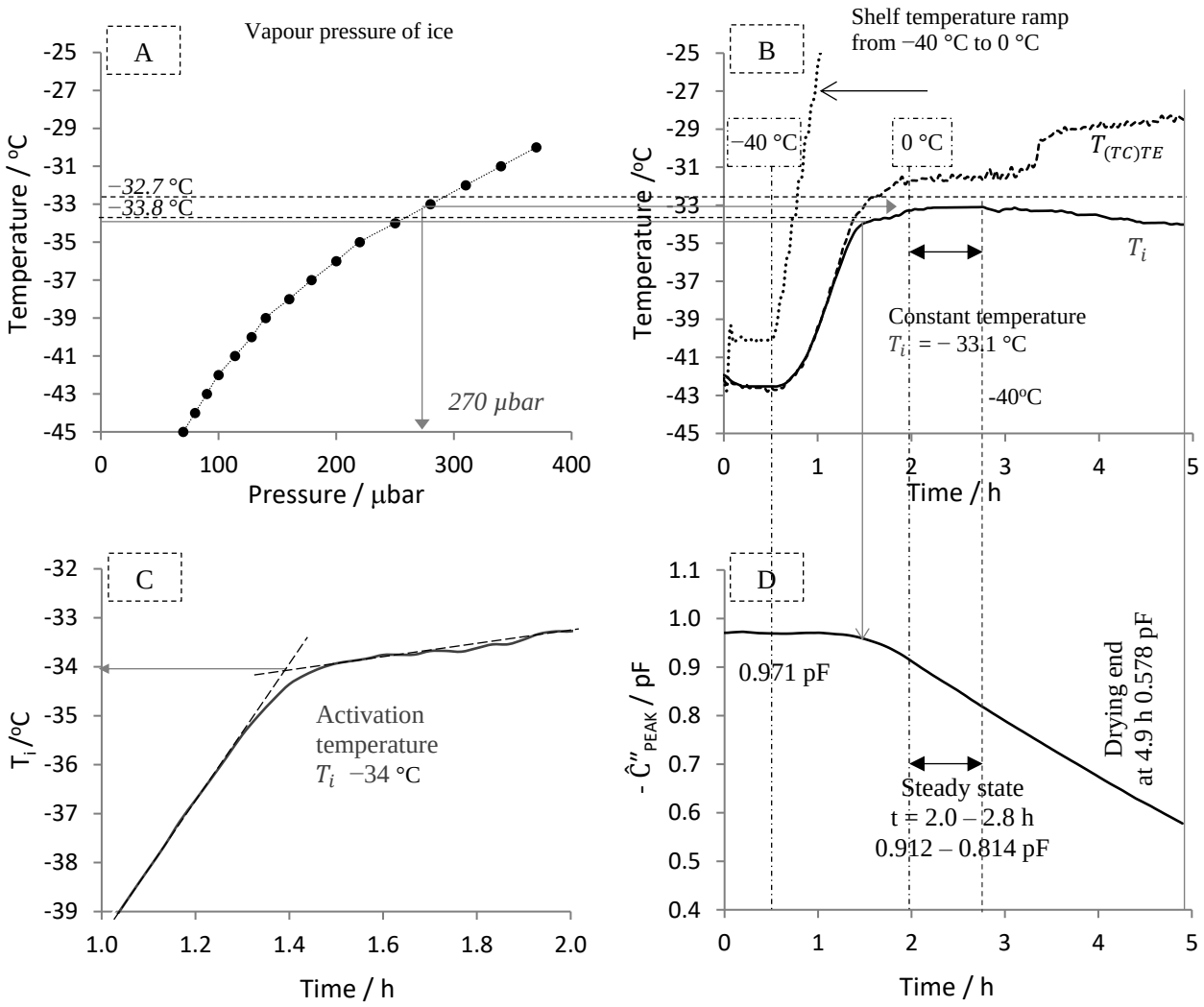

Figure 10. (A) Temperature dependency of the partial pressure of ice. The grey arrow demonstrates the anticipated temperature of the ice interface (−33.2 °C) when drying is activated by the condition whereby the partial pressure at the ice interface reaches a value equivalent to the pressure in the chamber (270 µbar), (B) Predicted ice interface temperature T_i(as determined by in Section 3.3) as a function of primary drying time. The constant temperature region between 2 and 2.8 h starts once the shelf temperature has reached its set temperature of 0 °C. During this time the predicted ice interface temperature is almost constant at -33.1 ±0.2 °C; (C) predicted ice interface temperature $T_i$close to the activation point when the drying rate starts to increase dramatically; (D) Temperature standardized values of $\hat{C}''_{PEAK}$. The plot also highlights those values at the beginning and end of the steady state period in which the drying rate is constant.

3.6 Qualification of drying rate predictions

One relatively straight forward way to qualify whether TVIS may be used to determine drying rates is to compare the average drying rate estimated from the change in the temperature standardized values of peak amplitude $\hat{C}''_{PEAK}$ with the average gravimetric drying rate determined

from the loss of ice mass at the end of the interrupted primary drying period.

As before, the first step is to calculate an average surrogate drying rate ($\Delta\hat{C}''_{PEAK}/\Delta t$) by taking the difference between $\hat{C}''_{PEAK}$ recorded before the temperature is ramped (0.971 pF) and $\hat{C}''_{PEAK}$ recorded at the end of the interrupted primary drying cycle (0.578 pF) then dividing by the time duration of the cycle (4.9 h) to give a value for $\Delta\hat{C}''_{PEAK}/\Delta t$ of 0.0804 pF/h.

The drying rate in g/h can then be calculated by using Eq. (5) which is reproduced here

$$\frac{\Delta m}{\Delta t} = \rho_i \cdot A \cdot m_{h/C} \cdot \frac{\Delta C''_{PEAK}}{\Delta t}$$

where ρ_i = 0.921 g cm^{-3} (i.e. the density of ice at an average ice cylinder temperature of −32 °C) [29], A = 3.80 cm^2 (calculated from the internal diameter of the Adelphi VC010-20C vial of 2.2 cm), and $m_{h/C}$ is 0.97485 cm/pF (from Fig. 6 in Section 3.3); to give a value for the TVIS predicted average drying rate of 0.274 g/h. This compares favorably with an average gravimetric drying rate of 0.25 g/h (from the loss of 1.22 g ice mass within 4.9 h). The 10% difference could be a result of the ice interface changing shape and hence surface area, with the height of the ice cylinder (i.e. that part in direct contact with the internal surface of the glass wall) reducing at a faster rate than the center of the ice interface, resulting in an increase in the relative height of the ice mass that sits as an ice cone on top of the aforementioned ice cylinder.

3.7 K_v Determination

An understanding of the heat transfer coefficient (K_v) between the heat source (i.e. the freeze-drying shelf) and the contents of the vial is essential if one is attempting to predict the behavior of large collections of vials within a batch scale freeze-dryer. With this new TVIS method and its application in a small scale dryer, we have demonstrated how to use a dual electrode pair, mounted on a single vial, to estimate the temperature at the base of the vial (T_b) while capturing the drying rate at the ice-interface ($\Delta m/\Delta t$). These two parameters (T_b and $\Delta m/\Delta t$) can then be combined to estimate K_v from Eq. (6) [27].

$$\frac{\Delta Q}{\Delta t} = L\frac{\Delta m}{\Delta t} = A_e K_V (T_s - T_b) \qquad (6)$$

where $\Delta Q/\Delta t$ is heating rate between the shelf and the base of the ice inside the TVIS vial, $\Delta m/\Delta t$ is the drying rate from the TVIS vial in g/h (as determined from Eq. (5), where the value for $\Delta \hat{C}''_{PEAK}/\Delta t$ is taken from the steady state period marked on Fig. 10D), L is the latent heat of sublimation of ice (2844 J·g^{-1}, or 679.7 Cal·g^{-1}), A_e is external cross-sectional area of the base of the TVIS vial in cm^2 and T_s is the shelf temperature in °C. Parameters for the calculation heat transfer coefficient at 270 µbar are given in Table 3.

Table 3. Parameters for the calculation heat transfer coefficient at 270 µbar

Parameters	**TVIS**
TVIS drying rate during steady state, g/h	*0.42*
Shelf temperature (T_s), °C	*0.14*
Ice base temperature (T_b) by TVIS, °C	*–29.8*
Heat transfer coefficient (K_V) at 270 µbar	
In units of W·m^{-2}·K^{-1}	*24.0*
In units of Cal·s^{-1}·cm^{-2}·K^{-1}	*5.73 × 10^{-4}*

Steady state is defined firstly by the condition that the TVIS determined product temperature, $T_{(F_{PEAK})}$, for both electrodes is constant (in practical terms this means that the both temperatures do not drift by more than 0.2 °C) and secondly by the condition that the instantaneous rate of change in TVIS derived sublimation rate does not change by more than ~5% from the start of steady-state to the end of steady-state. In practice the start of steady state coincides with the start of the constant temperature period for the shelf temperature.

4. Discussion

The estimate we have obtained for the heat transfer coefficient at the chamber pressure of 270 µbar (Table 3) agrees to within ~ 99.8 and 83.5% of those estimates determined by Tschessalov [1] and Brulls [30], respectively, for a comparable type of glass tubing vial (Fig. 11). However, the dryers used in those studies were clearly different in scale to the VirTis AdVantage Plus that we have used in

our work, and given that it has also been show that dryer design and scale also impacts individual $K_v$values (as does the method used for its determination) then it is hardly unsurprising that the there is some disagreement between the three sets of values. The fact that our K_v value compares favorably with that determined by Tschessalov [1] is yet another qualification that the TVIS method developed here is a valid approach for determining a suite of critical process parameters (i.e. $\Delta m/\Delta t$, T_i and T_b).

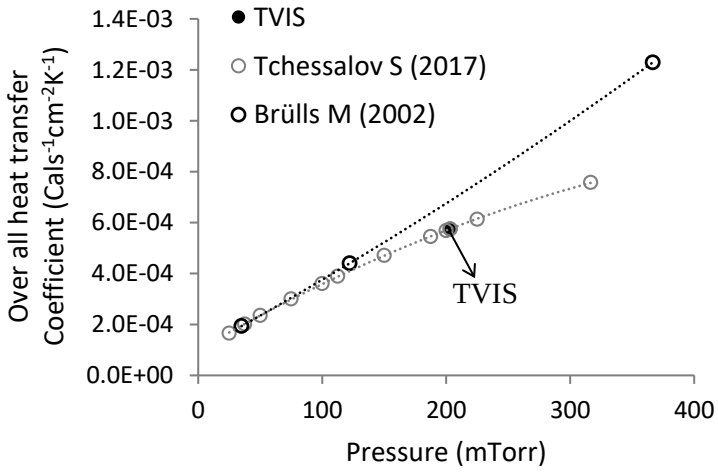

Figure 11. Comparison of the TVIS predicted estimate for the K_v value of a 10 mL glass tubing vial with previously published data for similar vials.

We have further validated our approach by being able to predict the ice interface temperature at which the partial pressure at the sublimation interface to a value which is equal to that of the chamber pressure. The precision of ~0.2 °C in the prediction of ice interface temperature also suggests a possible use of TVIS for tracking the collapse potential of a frozen solution during the primary drying stage of a freeze-drying cycle.

For this application (i.e. the determination of the heat transfer coefficient) it is recognized that with the current design of the dual electrode measurement system it is not possible to track the entire primary drying phase and instead we are limited to the determination of the drying conditions for first 40% loss of the frozen mass. This percentage of the frozen mass is a theoretical limit defined by the proportion of the total mass of ice in the vial that is within the linear response region of the ice which is bounded by the upper electrode. Given that the linear response region is associated with

fill factors between 0.13 to 0.7, or fill heights in the upper electrode region of 2 to 10.5 mm, and that the lower edge of the top electrode is positioned 10 mm above the internal base of the vial, then this linear response region represents a range of ice fill heights from 12 to 20.5, as measured from the internal base of the vial (i.e. a 40 % change in fill height and hence fill volume or mass).

However, the opportunity to measure as much as 40% of the ice mass lost during the sublimation process, is consistent with current industrial practice for a gravimetric approach to drying rate determination which recommends that drying is interrupted after ~ 20-25% of the ice mass is removed [27,31,32]. The primary reason for this limit is that one assumes that the shape of the ice interface and the contact of the ice with the walls of the vial won't have changed over this period and therefore the contributions from the various heat transfer mechanisms also won't have changed and therefore drying will have occurred at a constant rate.

One limitation of the TVIS technology is that the parameter $\hat{C}''_{PEAK}$ won't directly detect any change in the shape of the ice front. For example if the external length of the ice cylinder which intimately contact with the glass wall, decreases at a faster rate than the centre of the ice cylinder (Fig. 12) such that the ice mass develops a more substantive cone or domed shaped top surface (sublimation interface) then the TVIS determined drying rate will inevitably overestimate the true drying rate. This scenario is more likely for those vials closer to and at the edges of each shelf which receive an additional heat source from radiation. In order to avoid such errors in the drying rate determination then one should limit the period over which the steady state drying period is studied. For those vials at the edge the steady state period will be shorter than those vials at the core of the shelf. The key question is how to identify that part/period of the primary drying cycle over which there is minimal change in the profile of the sublimation interface.

With the TVIS approach one can use $\hat{C}''_{PEAK}$ as a direct measure of the instantaneous drying rate, at least in so far as the rate of drying of the ice cylinder in contact with the inside of the glass wall is concerned (see Fig. 12) and one can use the evidence of a constant drying temperature

($T_{(F_{PEAK})}$) and a constant drying rate (in so far as that predicted by TVIS) to qualify that it is unlikely that there has been any change in the contributions from the various heat transfer mechanisms.

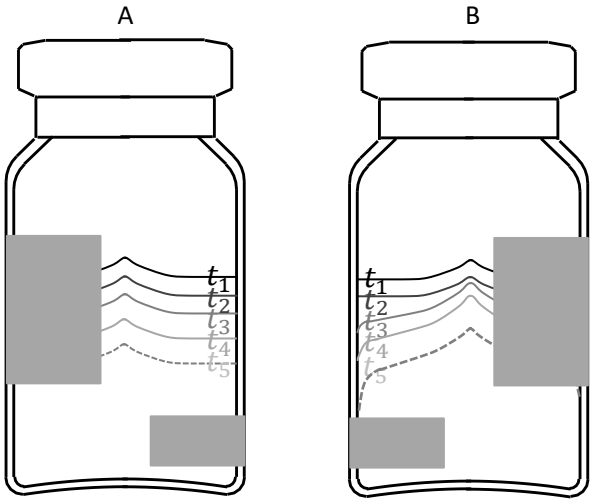

Figure 12. Two different scenarios for the shape of the sublimation interface at 5 equally spaced points (t_1 to t_5). (A) is the ideal scenario whereby the shape of the sublimation interface does not change throughout the primary drying cycle whereas (B) is the more typical pattern of changes to the sublimation shape during sublimation. At the beginning of primary drying (t_1 to t_2).the shape of ice layer does not change in both scenarios and therefore one expects C''_{PEAK} to be directly proportional to the ice mass. However, as drying proceeds (t_2 to t_5) the surface area of sublimation interface shown in scenario (B) starts to increase and an air gap develops between the ice and glass wall appears. Under those circumstances the relationship between C''_{PEAK} and ice mass will deviate from linear. Scenario (B) occurs routinely when drying ice however, the transition point between linear to non-linear will be reached sooner in the edge vial compared to the core vial.

Moreover, it appears that the time profile for F_{PEAK} might itself provide a clue as to the point at which there is a change in the curvature of the ice interface. The evidence is that during primary drying one expects the drying rate to decrease as the contact with the side wall degrades and the rate of heat transfer slows. The rate of self-cooling is reduced accordingly and so the temperature of the ice layer starts to increase. This phenomenon is picked up by the ice temperature that is sensed by the thermocouple placed at the bottom if the vial. However, as the thermocouple temperature starts to increase then the value of F_{PEAK} starts to decrease and so the downward trajectory of the F_{PEAK} profile has nothing to do with temperature but must be due instead to some change in the profile of the ice interface. In fact, as was pointed out in Section 3.6, the 10% discrepancy between the average gravimetric drying rate and the average TVIS drying rate suggests that a change in shape

of the ice interface is possible over the time period leading up to the point of interruption.

In an initial attempt to determine the possible mechanism, we consider how the equivalent electrical circuit model for the composite object of the glass vial and frozen contents (Fig. 13) might change when the ice begins to lose contact with the inside surface of the glass wall.

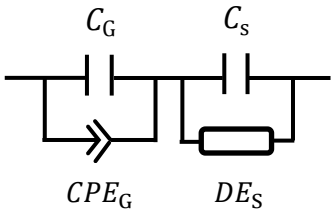

Figure 13. The equivalent circuit model for frozen water containing in vial. The left part of the model represents the impedance of the glass wall with the instantaneous polarization of glass being modelled by a capacitor (C_G) and the low frequency dispersive polarization of glass being as modelled by a constant phase element (CPE_G). The instantaneous capacitance of ice (C_s) and the dielectric relaxation of ice (DE_s) are demonstrated on the right part of the model.

The left side of the equivalent circuit consists of the capacitance of glass (C_G)in parallel with a constant phase element (CPE_G) which model, respectively, the instantaneous capacitance of glass and the low frequency dispersion associated with the percolation of charge through the porous matrix of fused silica glass. On the right side of the circuit the capacitor (C_s) models the high frequency (instantaneous capacitance) of ice whereas the distributed element (DE_s) models the dielectric relaxation of ice.

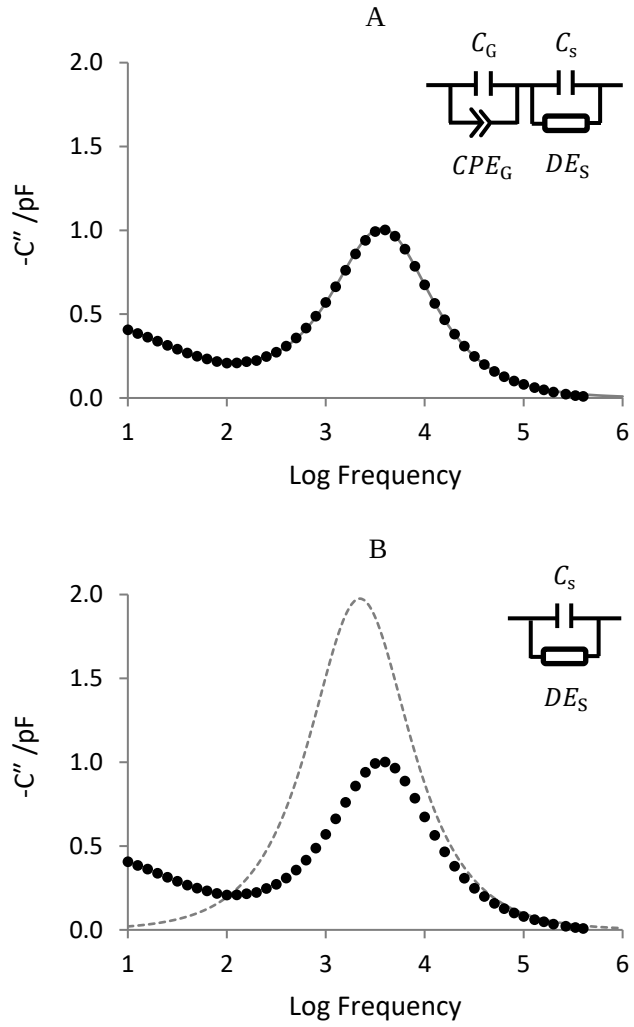

Figure 14. Equivalent circuit modelling of an example spectrum of ice. The data points are the measured values of the imaginary capacitance spectrum of ice at -20 °C during the re-heating part of the annealing stage. The solid line in (A) demonstrates the data fitted to the complete model (C_G=CPE_G-C_s=DE_s) *as shown in the top right. (B) shows the simulation results (dash line) when the glass wall impedance* (C_G and CPE_G) *has been removed from the completed model.*

The data points on Fig. 14 are the measured values for the TVIS imaginary capacitance spectrum for ice at -20 °C (during re-heating) and the solid line shows the data fit to the model that shown on the top right of each spectrum. In Fig. 14A the complete model has been fitted to the data (See Table 4 for the estimates of the fit parameters). In Fig. 14B the fitted parameters from Fig. 14A have been taken and those parameters relating to the glass wall impedance (C_G and CPE_G) have been removed and a simulation of the response from the impedance of the ice has been generated (see dash line on Fig. 14B). In other words Fig. 14B shows what one would expect to observe if it

were possible to measure the sample without the glass wall. One could therefore expect that the simulated response would be similar to the dielectric relaxation of ice [33]. It is clear that the glass wall shifts the relaxation peak to a higher frequency than that one would expect to see if ice were measured in the absence of the glass wall interface and therefore it might be the case that an air gap between the ice and the glass wall has the opposite effect, i.e. to partly return the relaxation peak back towards that expected for ice. And so we presume that the decrease in F_{PEAK} during primary drying at the point when the thermocouple suggests that the ice temperature is either constant or increasing is in fact a sign that some macroscopic structural change has occurred within the ice mass.

Table 4. The parameters from the fitting data of the re-heating ice at -20 °C to the model for frozen water (C_G=CPE_G-C_s=DE_s)

Fitting parameters	Fitting results
C_G	5.56×10^{-12}
CPE_G-T	4.68×10^{-11}
CPE_G-P	0.417
C_s	4.83×10^{-13}
DE_s-R	4.08×10^{-12}
DE_s-T	7.19×10^{-5}
DE_s-P	1.00
DE_s-U	0.980

Another potential issue with the application of the TVIS system for the determination of K_v relates to its use for the edge vials, which are thought to receive a high proportion of radiative heat transfer. Clearly if the electrode is in the line of sight of the radiation source then it would reflect rather than absorb the heat and therefore would introduce an error in the determination of K_v. In order to minimise the impact it would be prudent to ensure that the TVIS vial is orientated such that the intra electrode space, on the side wall, is directed towards the heat source. Given that the edge vial has one third (33%) of the vial circumference exposed to the radiation source and that the intra-vial spacing is one quarter (25%) of the vial circumference then up to 7% of the heat radiation that would reach the vial might be blocked by the electrode. That estimate, however, reduces by ~30% (from 7% to 5%) when one considers that the electrode does not extend to the base of the vial.

5. Conclusion

In this first exploration of the use of TVIS to determine the primary drying rate and the critical temperatures at the ice interface and ice base, we have demonstrated the potential for using TVIS as a process development tool for the determination of the heat transfer coefficient K_v at a single chamber pressure of 270 µbar.

6. Future work

Clearly there is a need to extend this work to encompass; (i) the determination of heat transfer coefficient as a function of chamber pressure and (ii) the investigation of the impact of vial size and shape [34]. Further work is also required in terms of the basic models used to understand the physical origin of the dielectric loss process that has been exploited in this work. Here we have used a simple polynomial function was to model the temperature dependency of the peak frequency. However, in future a more rigorous approach might be to fit the data with the Cole-Cole relaxation function to determine the relaxation time and to use the equations 15 and 16 in the work by Popov et al.[35] to provide a more substantive basis for defining the characteristics (i.e. saddle shape) of the calibration curve; one which takes into account the cross-over behavior in the polarization mechanism of ice, from orientation defect propagation at higher temperature (> 235 K) to ionic defect propagation at lower temperature (< 235 K).

7. Acknowledgement

De Montfort University acknowledges the support from the Technology Strategy Board Collaborative R&D grant LyoDEA (project reference: 100527) which facilitated the development of the TVIS process analytical technology that was used for this research. Yowwares Jeeraruangrattana is fund by the Government Pharmaceutical Organization (GPO), Thailand.

References

[1] S. Tchessalov, Application of modeling to lyophilization process design and scale up: process validation approaches. (2017).

[2] S. Rambhatla, M.J. Pikal, Heat and mass transfer scale-up issues during freeze-drying, I: atypical radiation and the edge vial effect, AAPS PharmSciTech 4 (2003) 22-31.

[3] S. Rambhatla, S. Tchessalov, M.J. Pikal, Heat and mass transfer scale-up issues during freeze-drying, III: control and characterization of dryer differences via operational qualification tests, AAPS PharmSciTech 7 (2006) E61-E70.

[4] D. Varshney, M. Singh, Lyophilized Biologics and Vaccines: Modality-Based Approaches., Springer, New York, 2015.

[5] A.A. Barresi, R. Pisano, D. Fissore, V. Rasetto, S.A. Velardi, A. Vallan, M. Parvis, M. Galan, Monitoring of the primary drying of a lyophilization process in vials, Chem. Eng. Process. 48 (2009) 408-423.

[6] N. Milton, M.J. Pikal, M.L. Roy, S.L. Nail, Evaluation of manometric temperature measurement as a method of monitoring product temperature during lyophilization, PDA J Pharm Sci Technol 51 (1997) 7-16.

[7] I. Oddone, D. Fulginiti, A.A. Barresi, S. Grassini, R. Pisano, Non-invasive temperature monitoring in freeze drying: control of freezing as a case study, Drying Technol. 33 (2015) 1621-1630.

[8] M. Parvis, S. Grassini, D. Fulginiti, R. Pisano, A.A. Barresi, Sputtered thermocouple array for vial temperature mapping (2014) 1465-1470.

[9] S. Schneid, H. Gieseler, Evaluation of a new wireless Temperature Remote Interrogation System (TEMPRIS) to measure product temperature during freeze drying, AAPS PharmSciTech 9 (2008) 729-739.

[10] S.C. Schneid, H. Gieseler, W.J. Kessler, M.J. Pikal, Non-Invasive Product Temperature Determination during Primary Drying using Tunable Diode Laser Absorption Spectroscopy, J. Pharm. Sci. 98 (2009) 3406-3418.

[11] S.M. Patel, M. Pikal, Process analytical technologies (PAT) in freeze-drying of parenteral products, Pharm. Dev. Technol. 14 (2009) 567-587.

[12] S. Nail, S. Tchessalov, E. Shalaev, A. Ganguly, E. Renzi, F. Dimarco, L. Wegiel, S. Ferris, W. Kessler, M. Pikal, Recommended best practices for process monitoring instrumentation in pharmaceutical freeze drying—2017, AAPS PharmSciTech 18 (2017) 2379-2393.

[13] D. Fissore, R. Pisano, A.A. Barresi, Process analytical technology for monitoring pharmaceuticals freeze-drying–A comprehensive review, Drying Technol. (2018) 1-27.

[14] X. Li, Nuclear Magnetic Resonance Imaging of Freeze-Drying, J. Pharm. Sci. 95 (11) 2516-2525.

[15] C.S. Song, J.H. Nam, C.J. Kim, S.T. Ro, Temperature distribution in a vial during freeze-drying of skim milk, J. Food Eng. 67 (2005) 467-475.

[16] H. Gieseler, W.J. Kessler, M. Finson, S.J. Davis, P.A. Mulhall, V. Bons, D.J. Debo, M.J. Pikal, Evaluation of tunable diode laser absorption spectroscopy for in-process water vapor mass flux measurements during freeze drying, J. Pharm. Sci. 96 (2007) 1776-1793.

[17] W.Y. Kuu, K.R. O'Bryan, L.M. Hardwick, T.W. Paul, Product mass transfer resistance directly determined during freeze-drying cycle runs using tunable diode laser absorption spectroscopy (TDLAS) and pore diffusion model, Pharm. Dev. Technol. 16 (2011) 343-357.

[18] W.Y. Kuu, S.L. Nail, G. Sacha, Rapid Determination of Vial Heat Transfer Parameters Using Tunable Diode Laser Absorption Spectroscopy (TDLAS) in Response to Step-Changes in Pressure Set-Point During Freeze-Drying, J. Pharm. Sci 98 (2009) 1136-1154.

[19] X.C. Tang, S.L. Nail, M.J. Pikal, Evaluation of manometric temperature measurement, a process analytical technology tool for freeze-drying: part II measurement of dry-layer resistance, AAPS PharmSciTech 7 (2006) E77-E84.

[20] X.C. Tang, S.L. Nail, M.J. Pikal, Evaluation of manometric temperature measurement (MTM), a process analytical technology tool in freeze drying, part III: heat and mass transfer measurement, AAPS PharmSciTech 7 (2006) E105-E111.

[21] W.Y. Kuu, L.M. Hardwick, M.J. Akers, Rapid determination of dry layer mass transfer resistance for various pharmaceutical formulations during primary drying using product temperature profiles, International Journal of Pharmaceutics 313 (2006) 99-113.

[22] A.A. Barresi, S.A. Velardi, R. Pisano, V. Rasetto, A. Vallan, M. Galan, In-line control of the lyophilization process. A gentle PAT approach using software sensors, Int. J. Refrig. 32 (2009) 1003-1014.

[23] G. Smith, M.S. Arshad, E. Polygalov, I. Ermolina, T.R. McCoy, P. Matejtschuk, Process understanding in freeze-drying cycle development: applications for through-vial impedance spectroscopy (tvis) in mini-pilot studies, J Pharm Innov 12 (2017) 26-40.

[24] G. Smith, E. Polygalov, M. Arshad, T. Page, J. Taylor, I. Ermolina, An impedance-based process analytical technology for monitoring the lyophilisation process, Int. J. Pharm. 449 (2013) 72-83.

[25] M.S. Arshad, G. Smith, E. Polygalov, I. Ermolina, Through-vial impedance spectroscopy of critical events during the freezing stage of the lyophilization cycle: the example of the impact of sucrose on the crystallization of mannitol, Eur. J. Pharm. Biopharm. 87 (2014) 598-605.

[26] G. Smith, M.S. Arshad, E. Polygalov, I. Ermolina, An application for impedance spectroscopy in the characterisation of the glass transition during the lyophilization cycle: the example of a 10% w/v maltodextrin solution, Eur. J. Pharm. Biopharm 85 (2013) 1130-1140.

[27] M. Pikal, M. Roy, S. Shah, Mass and heat transfer in vial freeze-drying of pharmaceuticals: Role of the vial, J. Pharm. Sci. 73 (1984) 1224-1237.

[28] G. Smith, E. Polygalov, T. Page, Electrical Monitoring of a Lyophilization Process (2011).

[29] Å Melinder, Properties and other aspects of aqueous solutions used for single phase and ice slurry applications, Int. J. Refrig. 33 (2010) 1506-1512.

[30] M. Brülls, A. Rasmuson, Heat transfer in vial lyophilization, Int. J. Pharm. 246 (2002) 1-16.

[31] S. Hibler, C. Wagner, H. Gieseler, Vial freeze-drying, part 1: New insights into heat transfer characteristics of tubing and molded vials, J. Pharm. Sci. 101 (2012) 1189-1201.

[32] B. Scutella, S. Passot, E. Bourles, F. Fonseca, I.C. Trelea, How Vial Geometry Variability Influences Heat Transfer and Product Temperature During Freeze-Drying, J. Pharm. Sci. 106 (2017) 770-778.

[33] I. Popov, I. Lunev, A. Khamzin, A. Greenbaum, Y. Gusev, Y. Feldman, The low-temperature dynamic crossover in the dielectric relaxation of ice I h, Phys. Chem. Chem. Phys. 19 (2017) 28610-28620.

[34] B. Scutellà, A. Plana-Fattori, S. Passot, E. Bourlès, F. Fonseca, D. Flick, I. Trelea, 3D mathematical modelling to understand atypical heat transfer observed in vial freeze-drying, Appl. Therm. Eng. 126 (2017) 226-236.

[35] I. Popov, A. Puzenko, A. Khamzin, Y. Feldman, The dynamic crossover in dielectric relaxation